Modelling spread risk via time change approach

Andrea Giustini

University of Rome La Sapienza
andrea.giustini@uniroma1.it

Abstract

This paper considers a stochastic model for managing spread risk by time changing the jump Cox-Ingersoll-Ross (JCIR) process with a random clock, which has a mean reverting jump component that leads to mean reversion in the level of credit spread in addition to the smooth mean reversion force. In order to calibrate the model we use the particle filtering technique, which allows for the estimate of real-world and risk-neutral probability distributions from time series of credit spread observations.

I. Introduction

Directive 2009/138/CE of the European parliament and of the council (Solvency II) requires insurance companies to have a level of Own Funds consistent with the risks to which they are exposed, at least equal to Solvency Capital Requirement (SCR), which is defined as the Value-at-Risk (VaR) of the one-year distribution of the company's Basic Own Funds (BOF), with a probability level of 99.5%.

The approaches proposed for calculating the SCR include, among others, the Standard Formula - a predefined model calibrated on data relating to the European insurance market - and the Internal Model, which should represent undertaking risk profile as accurately as possible. Both approaches require that balance sheet items should be evaluated according to a market consistent method. Therefore, in accordance with the principles of the Directive, valuation of BOF is carried out using risk-neutral probabilities and, on the other hand, valuation of VaR of the one-year distribution of the company's BOF should be based on real-world probabilities of risk factors affecting BOF. In order to comply Directives principles, calibration of the models should be carried out on the basis of time series of market values, from which both probability distributions can be inferred.

Among the risks covered by SCR, in this paper we analyzed spread risk, defined as "the sensitivity of the values of assets, liabilities and financial instruments to changes in the level or in the volatility of credit spreads over the risk-free interest rate term structure"[1] . Although many factors can affect the level or the volatility of credit spread, such as counterparty risk, tax effects and liquidity risk (Elton et al. 2001, Dignan 2003 and Driessen 2003), we assume that only counterparty risk is relevant, leaving other components as residuals. Counterparty risk can be defined as the risk that, in the context of a credit transaction, a debtor fails to meet his obligations (repay the principal and/or interest), even partially. The additional return required by the creditor, i.e. the risk premium for default risk, is composed by arrival risk, timing risk, and recovery risk (Schönbucher 2003). Arrival risk is a term for the uncertainty whether a default will occur or not; timing risk refers to the uncertainty about the precise time of default; recovery risk describes the uncertainty about the severity of the losses if a default has happened.

[1] Article 105 of the Directive.

Considering the above assumptions, in order to manage spread risk we use an intensity-based model, developed by Li et al. 2016 in the context of electricity spot price modelling, properly adapted to model counterparty risk. Set up within the one-dimensional Markovian framework, the model is based on the Cox-Ingersoll-Ross (CIR) diffusion process, interspersed with compound Poissons jumps with exponentially distributed jump size and a subordinated process as a random clock. These results allow to obtain both tractability and interesting features in sample paths: process' jumps are state-dependent and contribute to the return to the long-time average level, together with the mean-reversion drift component.

Estimation on market data of the model parameters is carried out through maximum likelihood estimation (MLE), where the likelihood function is calculated via particle filter technique (Bolviken and Storvik 2001); this approach allows to estimate both probability distributions as a whole.

The rest of this paper is organized as follow. Section (**2**) describes the modelling framework. Section (**3**) provides a brief description of the general theory of filtering; in this section we introduce the filter and we mention the situations in which particles are necessary. In section (**4**) we apply the particle filtering technique to calibrate the model; here we analyze the results of the calibration phase by comparing some statistics related to the market and model time series.

II. Spread risk model

The model. Let (Ω, $\mathfrak{F}$, $\mathbb{P}$) a probability space equipped with a filtration $\{\mathcal{F}_t\}_{t\geq 0}$, such that $\forall t$ $\mathcal{F}_t \subset \mathfrak{F}$ and, for $s < t$ we have $\mathcal{F}_s \subset \mathcal{F}_t$. We define $\mathbb{P}$ as the real-world probability.

Under (Ω, $\mathfrak{F}$, $\mathbb{P}$), we model the instantaneous default intensity as:

$$\lambda_t^{\phi} = \lambda_{T_t} \tag{1}$$

where $(\lambda_t)_t$ is a JCIR process and T_t is a random clock.

A JCIR process is the unique solution to the following SDE:

$$d\lambda_t = \alpha(\gamma - \lambda_t)dt + \rho\sqrt{\lambda_t}dZ_t^{\mathbb{P}} + dJ_t \tag{2}$$

where $\alpha, \gamma, \rho > 0$ and $\lambda_0 = \lambda(0) > 0$. We also impose the Feller condition $2\alpha\gamma \geq \rho^2$, so that zero is an unattainable boundary for $(\lambda_t)_t$; $(J_t)_t$ is a compound Poisson process, independent from $(Z_t)_t$, with arrival rate $\omega > 0$ and the jump size which follows an exponential distribution with mean $\mu > 0$.

We choose the random clock T_t as an additive subordinator, i.e. a non-negative and non-decreasing additive process (Sato 1999). In particular, let T_t be a Gamma process (Madan, Carr, and Chang 1998), independent from $(\lambda_t)_t$; its Lévy measure is given by:

$$\nu(d\tau) = \frac{m^2/v}{\tau} e^{-\frac{m}{v}\tau} d\tau, \tag{3}$$

where $m = \mathbb{E}[T_1] - \gamma_T$ and $v = \text{Var}[T_1]$ are the mean and variance rate of the stochastic part of the Gamma process respectively, while $\gamma_T \geq 0$ is the drift of T. In the rest of this paper, we adopt the following parametrization:

$$\nu(d\tau) = \frac{C}{\tau} e^{-\eta\tau} d\tau, \tag{4}$$

where $C = \dfrac{m^2}{v}$ and $\eta = \dfrac{m}{\nu}$.

The Laplace transform of the Gamma process is given by:

$$\mathbb{E}[e^{-wT_t}] = e^{\psi(w)t}, \tag{5}$$

with the Laplace exponent:

$$\psi(w) = w\gamma_T + C\ln(1 + \frac{w}{\eta}). \tag{6}$$

Following Li et al. 2016, we call $(\lambda_t^{\phi})_t$ "GMAC-JCIR process". We now calculate the Laplace transform of the GMAC-JCIR process $(\lambda_t^{\phi})_t$.

First, the Laplace transform of the JCIR process $(\lambda_t)_t$ is well known (Duffie and Singleton 1999):

$$\mathbb{E}_\lambda[e^{-z\lambda_t}] = C(z,t)A(z,t)e^{-B(z,t)\lambda}, \quad (7)$$

where:

$$C(z,t) = (e^{-\alpha t} + \frac{(2\alpha + z\rho^2)(1-e^{-\alpha t})}{2\alpha(1+z\mu)})^{-\omega a}, \quad (8)$$

$$B(z,t) = \frac{2\alpha z}{2\alpha + (2\alpha + z\rho^2)(e^{\alpha t}-1)}, \quad (9)$$

$$A(z,t) = (\frac{2\alpha e^{\alpha t}}{2\alpha + (2\alpha + z\rho^2)(e^{\alpha t}-1)})^b, \quad (10)$$

and

$$a = \frac{2\mu}{\rho^2 - 2\mu\alpha}, \quad b = \frac{2\alpha\gamma}{\rho^2}. \quad (11)$$

Therefore, the Laplace transform of $(\lambda_t^\phi)_t$ can be written as:

$$\mathbb{E}[e^{-z\lambda^\phi}] = \int_0^{+\infty} \mathbb{E}_x[e^{-z\lambda_u}]q_{s,t}(du). \quad (12)$$

Now, let $g_t(du)$ be the transition probability distribution of a Gamma subordinator with zero drift, mean and variance rate m and ν, then $g_t(du)$ is given by the following Gamma distribution:

$$g_t(du) = \frac{\eta^{Ct}}{\Gamma(C)}u^{Ct-1}e^{-\eta u}du \quad (13)$$

Equation (12) can be rewritten as:

$$\mathbb{E}[e^{-z\lambda^\phi}] = \int_0^{+\infty} \mathbb{E}_x[e^{-z\lambda_{\gamma_T(t-s)+u}}]g_{t-s}(du) \quad (14)$$

The integral (14) can be efficiently computed by the Gauss-Laguerre quadrature. A high level of accuracy can be obtained with a small number of quadrature points.

Availability of the Laplace transform of λ_t^ϕ allows to recover the transition probability density of the process through an efficient numerical Laplace inversion algorithm.

Equivalent measure change for GMAC-JCIR process. It can be shown that $(\lambda_t^\phi)_t$ is a Markov semimartingale on (Ω, $\mathfrak{F}$, $\mathbb{P}$). Li et al. 2016 derive general explicit conditions under which $(\lambda_t^\phi)_t$ is Markov semimartingale on (Ω, $\mathfrak{F}$, $\mathbb{Q}$), where $\mathbb{Q}$ a probability measure equivalent to $\mathbb{P}$.

In general, for the tempered stable family of Lévy subordinators - which includes the Gamma process as a special case - the Lévy measure $\nu(d\tau)$ is given by:

$$\nu(d\tau) = C\tau^{-1-p}e^{-\eta\tau}d\tau \quad (15)$$

Let $(\hat{\alpha}, \hat{\gamma}, \hat{\rho}, \hat{\omega}, \hat{\mu}, \hat{C}, \hat{p}, \hat{\eta}, \hat{\gamma})$ be the parameters which identifies the probability distribtion of λ_t^ϕ under $\mathbb{Q}$, when the random clock belongs to the tempered stable family of Lévy subordinator. Suppose the following conditions are satisfied:

- $\hat{p} = p$
- $\hat{\gamma}\hat{\rho}^2 = \gamma\rho^2$
- $\hat{C}\hat{\rho}^{2\hat{p}} = C\rho^{2p}$

Then $\mathbb{Q}_{|\mathcal{F}_t} \sim \mathbb{P}_{|\mathcal{F}_t}$ for every $t \geq 0$ (Li et al. 2016).

Pricing under counterparty risk. In a market model defined with a probability space (Ω, $\mathfrak{F}$, $\mathbb{P}$) equipped with a filtration $\{\mathcal{F}_t\}_{t\geq 0}$, the value at time t of a contract X with maturity in T is:

$$\begin{aligned} X_t = \mathbb{E}^{\mathbb{Q}}\{&e^{-\int_t^T r_u du}\mathbf{1}_{\{\kappa > T\}}X_T \\ &+ e^{-\int_t^\kappa r_u du}\mathbf{1}_{\{\kappa \leq T\}}g_\kappa|\mathcal{F}_t\} \end{aligned} \quad (16)$$

where $\mathbb{Q}$ is a martingale measure equivalent to $\mathbb{P}$, κ is the instant of default, $\mathbf{1}_A$ is the indicator function of event A, g_κ is the value of the contract in case of default, and the spot rate $(r_t)_t$ uniquely determines term structure of interest rates. Assuming that g_κ is a deterministic fraction δ (Recovery Rate) of the value of the contract at the instant immediately preceding the default:

$$g(\kappa) = \delta X_{\kappa^-} \qquad \delta \in [0,1) \quad (17)$$

The price of the contract can be rewritten as (Duffie and Singleton 1999):

$$X_t = \mathbb{E}^{\mathbb{Q}}\{e^{-\int_t^T \left[r_u+(1-\delta)\lambda_u^{\phi}\right]du} X_T|\mathcal{G}_t\}, \quad (18)$$

where λ_u^{ϕ} is the default intensity.

Now, let $v(t,t+\tau)$ be the value at time t of a unit risk-free *zero-coupon bond* with maturity $t+\tau$ and $v^R(t,t+\tau)$ the value at time t of a risky *zero-coupon bond*, issued by an issuer with rating R, with maturity $t+\tau$ and conditional on the issuer not going bankrupt in $[0;t]$. From (18), assuming independence beetween interest rate risk and counterparty risk, we have:

$$\begin{aligned} v^R(t,t+\tau) &= \mathbb{E}^{\mathbb{Q}}\{e^{-\int_t^{t+\tau} \left[r_u+(1-\delta)\lambda_u^{\phi}\right]du}|\mathcal{F}_t\} \\ &= v(t,t+\tau)\mathbb{E}^{\mathbb{Q}}\{e^{-\int_t^{t+\tau}(1-\delta)\lambda_u^{\phi}du}|\mathcal{F}_t\} \end{aligned} \quad (19)$$

And the yield-to-maturity intensities for the maturity $t+\tau$ are given by:

$$h(t,t+\tau) = -\frac{1}{\tau}\log v(t,t+\tau) \quad (20)$$

$$h^R(t,t+\tau) = -\frac{1}{\tau}\log v^R(t,t+\tau) \quad (21)$$

Therefore, credit spreads can be defined as follows:

$$\begin{aligned} \bar{s}^R(t,t+\tau) &= h^R(t,t+\tau) - h(t,t+\tau) \\ &= -\frac{1}{\tau}\mathbb{E}^{\mathbb{Q}}\{e^{-\int_t^{t+\tau}(1-\delta)\lambda_u^{\phi}du}|\mathcal{F}_t\} \\ &:= -\frac{1}{\tau}Q(t,t+\tau) \end{aligned} \quad (22)$$

for every t and $\tau > 0$. In the rest of this paper, we omit the reference R of the rating for credit spreads.

III. Particle filtering technique

General issues. State space modelling provides a unified methodology for treating a wide range of problems in time series analysis. It is assumed that the development over time of a dynamic system is determined by an unobserved series of quantities with which are associated a series of observations, where the relation between the unobserved and the observed ones is specified by the state space model. In general, the main purpose of state space analysis is to infer the relevant properties of unobserved quantity from the characteristics of the observations (Durbin and Koopman 2001)

In our framework, the dynamic system for which measurements are available is represented by the market, where the measurements can happen in discrete time instants. From the independence between interest rates and credit spread, at every time the state of the dynamic system is determined only via the instantaneous default intensity: in this way, changes in the dynamic system are governed by real-world probability distribution of the instantaneous default intensity, while the risk-neutral probability distribution allows to take into account the relationship between the state of the system and the measurements, i.e. the observed credit spreads.

Filtering in state-space models concerns computing a series of linked numerical integrals, where output from one is input to the other (Bucy and Senne 1971). Particle filtering, in particular, can be regarded as a technique for solving these integrals by discrete approximations, based on particles (Kitagawa 1996). In the following we only consider the case of deterministic particle filtering. In contrast to Monte-Carlo filtering, it could be the preferred method when the state process has low dimension and high numerical accuracy is desired (Bolviken and Storvik 2001).

Exact filter. Suppose we deal with a Markov stochastic process $(\lambda_t^{\phi})_t$, observed indirectly through a discrete-time process:

$$(\mathbf{s_t^{obs}})_\mathbf{t} := (s^{obs}(t,t+\tau))_t \quad (23)$$

for some $\tau > 0$. We also define:

$$\mathbf{s^{obs}_{t_1:T}} := \{s^{obs}(t_1, t_1+\tau), ..., s^{obs}(T, T+\tau)\} \tag{24}$$

Let $p(\lambda^{\phi}_t|\lambda^{\phi}_{t-1})$ be the state equation, which represents the trasition probability distribution of the state variable λ^{ϕ}_t and describes the dynamic characteristics of the system at time t. The state equation is governed by the real-world probability distribution.

Let $p(\mathbf{s_t}|\lambda^{\phi}_t)$ be the observation equation, which represents the likelihood and describes the relationship between the latent variable and the observed ones at time t. The observation equation is governed by risk-neutral probability distribution.

The exact filter for the process $(\lambda^{\phi}_t)_t$ can be written as a set of recursive integration equations. Starting with:

$$p(\lambda^{\phi}_0|\mathbf{s_0}) := p(\lambda^{\phi}_0) \tag{25}$$

as the prior distribution of the state variable at time $t = 0$, we can calculate recursively:

$$\begin{aligned} &p(\lambda^{\phi}_t|\mathbf{s_{1:t-1}}) \\ &= \int_{\Re^+} p(\lambda^{\phi}_t|\lambda^{\phi}_{t-1}) p(\lambda^{\phi}_{t-1}|\mathbf{s_{1:t-1}}) d\lambda^{\phi}_{t-1}, \end{aligned} \tag{26}$$

$$\begin{aligned} &p(\lambda^{\phi}_t|\mathbf{s_{1:t}}) \\ &= C_t^{-1} p(\mathbf{s_t}|\lambda^{\phi}_t) p(\lambda^{\phi}_t|\mathbf{s_{1:t-1}}) \end{aligned} \tag{27}$$

for $t \geq 1$. The normalisation constants C_t is defined as follows:

$$C_t = \int_{\Re^+} p(\mathbf{s_t}|\lambda^{\phi}_t) p(\lambda^{\phi}_t|\mathbf{s_{1:t-1}}) d\lambda^{\phi}_t \tag{28}$$

and produces the log-likelihood function of the observations $(\mathbf{s_t})_\mathbf{t}$ through:

$$\log(p(\mathbf{s_{1:T}})) = \sum_{t=1}^{T} \log(C_t) \tag{29}$$

Deterministic particle filter. Computation of the integral in equations (26), (27) and (28) can be difficult. When all distributions are Gaussian and the relationship between the observed variables and the latent one is represented by a linear function, then there are closed-form solutions to the recursive equations (Kalman 1960, Kalman and Bucy 1961, Kalman and Bucy 1963). In general, when the integrals must be calculated with numerical techniques or the relationship is not linear, the recursive equations do not admit a closed-form solution. In this case we must deal with particle filter, a methodology that allows to calculate numerically the integrals through discrete approximations, based on the definition of points (particles) over the integration set.

In the context of deterministic particle filter, i.e. when the points are defined through a non-stochastic approach, evaluations of integrals can be efficiently carried out by Gaussian quadrature. The simplest among these rules is the Gauss-Legendre method (Golub and Welsch 1969). In this way, quadrature filters are constructed by replacing the densities in (26) and (27) by a particle approximation based on the quadrature formulas.

Let ${}_{(i)}\lambda^{\phi}_t$ be the particles (abscissas) defined over the integration set and ${}_{(i)}\epsilon$ be the correspondent positive wheigts, for $i = 1, ..., N$. Since with the particle filter we replace a continuous random variable with a discrete one, if $\hat{p}$ is some discrete analogue to the exact density p, we have the following recursive scheme:

$$\begin{aligned} &\hat{p}({}_{(i)}\lambda^{\phi}_t|\mathbf{s_{1:t-1}}) \\ &\quad = \sum_{j=1}^{N} p({}_{(i)}\lambda^{\phi}_t|{}_{(j)}\lambda^{\phi}_t) \hat{p}({}_{(j)}\lambda^{\phi}_{t-1}|\mathbf{s_{1:t-1}}) \end{aligned} \tag{30}$$

$$\begin{aligned} &\hat{p}({}_{(i)}\lambda^{\phi}_t|\mathbf{s_{1:t}}) \\ &\quad = \frac{p(\mathbf{s_t}|{}_{(i)}\lambda^{\phi}_t)\ {}_{(i)}\epsilon\ \hat{p}({}_{(i)}\lambda^{\phi}_t|\mathbf{s_{1:t-1}})}{\hat{C}_t} \end{aligned} \tag{31}$$

for $t \geq 1$, $i = 1, ..., N$ and:

$$\hat{C}_t = \sum_{i=1}^{N} p(\mathbf{s_t}|{}_{(i)}\lambda^{\phi}_t)\ {}_{(i)}\epsilon\ \hat{p}({}_{(i)}\lambda^{\phi}_t|\mathbf{s_{1:t-1}}) \tag{32}$$

$$\hat{p}({}_{(i)}\lambda_0^{\phi}|\mathbf{s_0}) = {}_{(i)}\epsilon p({}_{(i)}\lambda_0^{\phi}) \tag{33}$$

Then, the approximate likelihood function is defined as:

$$\log \hat{p}(\mathbf{s_{1:t}}) = \sum_{k=1}^{t} \log \hat{C}_k \tag{34}$$

IV. Model calibration

Calibration procedure. The calibration procedure consists of maximization of the likelihood function (34), which depends on parameters of both probability distributions. Therefore, the calibration procedure can be defined as:

$$\underset{\psi \in \Psi}{max} \log(\hat{p}(\mathbf{s_{1:t}})) \tag{35}$$

where $\psi = (\psi^{\mathbb{P}}, \psi^{\mathbb{Q}})$.

The state equation $p(\lambda_t^{\phi}|\lambda_{t-1}^{\phi})$ is derived by Laplace inversion of (14), through the algorithm proposed by Abate and Whitt 1992. By Li et al. 2016, we note that the parameters of the GMAC-JCIR model are identified up to a constant. Hence, in our calibration procedure we set $\gamma_T = 1$ for the jump-diffusion specification to fix the scale. Then, the state equation depends on real-world parameters, identified by:

$$\psi^{\mathbb{P}} = (\alpha, \gamma, \rho, \omega, \mu, m, \nu) \tag{36}$$

On the other hand, we assume for the observation equation $p(\mathbf{s_t}|\lambda_t^{\phi})$ a Gaussian distribution:

$$p(\mathbf{s_t}|\lambda_t^{\phi}) \sim N(\bar{\mathbf{s}}_t, \Sigma) \tag{37}$$

where $\bar{\mathbf{s}}_t$ is defined by (22) and Σ is a diagonal matrix, $\Sigma = \sigma^2 I$. For the GMAC-JCIR process the quantity Q in (22) cannot be obtained in closed form, so the credit spreads $\bar{\mathbf{s}}_t$ can be derived through Monte-Carlo simulation (Li et al. 2016). The observation equation depends on risk-neutral parameters, identified by:

$$\psi^{\mathbb{Q}} = (\hat{\alpha}, \hat{\gamma}, \hat{\rho}, \hat{\omega}, \hat{\mu}, \hat{m}, \hat{\nu}, \sigma^2) \tag{38}$$

We set $\psi^{\mathbb{P}}$ and $\psi^{\mathbb{Q}}$ in order to meet the conditions for which $\mathbb{Q}_{|\mathcal{F}_t} \sim \mathbb{P}_{|\mathcal{F}_t}$.

For the maximization problem, we assume the following:

- $P(\lambda_t^{\phi} \in [0, 0.05]) \sim= 1$;
- Over the integration set $[0, 0.05]$, we define $N = 128$ particles for the Gauss-Legendre method;
- $\lambda_0^{\phi} \sim Unif[0; 0.05]$.

The calibration procedure is implemented in R. For the solution of the optimum is used the library "nloptr", in particular the derivative-free algorithm Cobyla (Constrained Optimization By Linear Approximations) proposed by Powell 2007. The choice is justified by the fact that the likelihood function is very irregular and a gradient optimization algorithms do not allow stability of the solution. The maximum number of iterations has been set equal to 1000.

Calibration example. We calibrate our model on daily term structure of credit spreads from Bloomberg, belonging to the "A" rating class and the "finance" sector, from July 1, 2009 to December 30, 2016, and for maturities equal to 1, 2, 3, 4, 5, 6, 7, 8, 9 and 10 years.

Figure 1 shows that the correlation is very high between the spreads when maturities are near, while it decreases when credit spreads with short and long maturities are considered.

Calibration results. Results of the maximization problem (35) are displayed in tables 1 and 2). It can be noted that the real-world estimate is located on the boundary of the parameter space, i.e. we have $\dfrac{2\alpha\gamma}{\rho^2} \sim= 1$.

The estimate of the parameters of the model allows to estimate the state variable λ_t^{ϕ} for each $t \geq 1$, as the expected value of the (approximated) posterior distribution $\hat{p}(\lambda_t^{\phi}|\mathbf{s_{1:t}})$ (figure 2), that allows for calculation of model credit spread over the entire time horizon, via (22).

In figures 3, 4, 5 and 6, model and market values of credit spreads are reported for a set of maturities. It can be seen that the filter produces good results; however for lower and higher maturities the adaptation is less precise. In fact, a model which is governed by a unique factor allows for constant correlations among the term structure, unlike what is observed in the market.

Mean and variance analysis is reported in tables 3 and 4, and in figures 7 and 8, where several model and market statistics are compared.

In figures 9, 10, 11 and 12, distributions of residuals for a set of maturities are reported, while qq-plots of residuals are displayed in figures 13, 14, 15 and 16. It can be seen that residuals are inconsistent with the hypothesis of Gaussian distribution.

The overall prediction error is measured by the Root Mean Squared Error (RMSE), defined as follows:

$$RMSE = \sqrt{\frac{1}{N}\sum_{i=1}^{N} e_i^2}, \tag{39}$$

where $e_i = \bar{\mathbf{s}}_\mathbf{i} - \mathbf{s}_\mathbf{i}$. Results are reported in table 5 for all maturities. The goodness of fit of the model is better when central maturities are considered.

V. Conclusions

Results show the goodness of the estimates made by particle filtering technique: data used for calibration are satisfactory reproduced by the model, especially when intermediate maturities are considered.

The implementation of the particle filtering also affects the speed and the stability of the solution. Further analysis involves the dependence of the solution on the time series and with respect to the local mimima of the likelihood function.

References

References

Abate and Whitt (1992). "The Fourier-series method for inverting transforms of probability distributions". In: *Queueing Syst.*

Bolviken and Storvik (2001). "Deterministic and Stochastic Particle Filters in State-Space Models". In: *Sequential Monte Carlo Methods in Practice*. Springer. Chap. 5, pp. 97–116.

Dignan (2003). "Nondefault components of investment-grade bond spread". In: *Financial Analysts Journal*.

Driessen (2003). "Is default event risk priced in corporate bonds?" In: *Financial Analysts Journal*.

Duffie and Singleton (1999). "Modelling term structure of defoultable bond". In: *The Review of Financial Studies*.

Durbin and Koopman (2001). *Time Series Analysis by State Space Methods*. Oxford University Press.

Elton et al. (2001). "Explaining the rate spread on corporate bond". In: *The Journal of Finance*.

Golub and Welsch (1969). "Calculation of Gauss quadrature rules". In: *Math. Comp.*

Kalman (1960). "A new approach to linear filtering and prediction problems". In: *Trans. ASME*.

Kalman and Bucy (1961). "New result in lenear filtering and prediction theory". In: *Trans. ASME*.

– (1963). "New methods in wiener filtering theory". In: *Proc. Symp. Appl. Random Function Theory and Probability*.

Li et al. (2016). "Modelling electricity prices: a time change approach". In: *Quantitative Finance*.

Madan, Carr, and Chang (1998). *The variance Gamma process and option pricing*. Eur. Finance Rev.

Powell (2007). "A view of algorithms for optimization without derivatives". In: *Cambridge University Technical Report*.

Sato (1999). *Lévy Processes and Infinitely Divisible Distributions*. Cambridge University Press.

Schönbucher (2003). *Credit derivatives pricing models: models, pricing and implementation*. Wiley.

Tables and figures

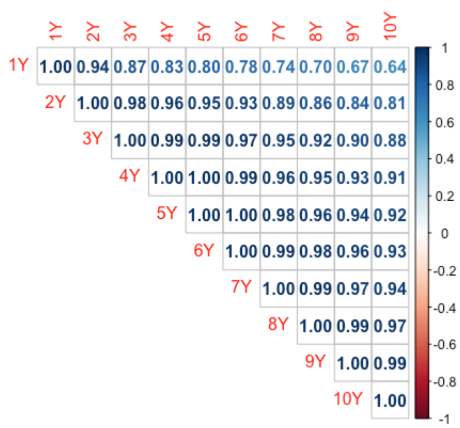

Figure 1: Correlation of market credit spreads

Table 1: Estimation result for the model

	Estimate
α	0.17
γ	0.00318
ρ	0.0325
ω	31.37
μ	0.00018
C	2.77
η	0.1718

Table 2: Estimation result for the model

	Estimate
$\hat{\alpha}$	0.03999
$\hat{\gamma}$	0.08744
$\hat{\rho}$	0.0325
$\hat{\omega}$	0.05236
$\hat{\mu}$	0.02513
$\hat{C}$	2.77
$\hat{\eta}$	14.716
σ	0.0012

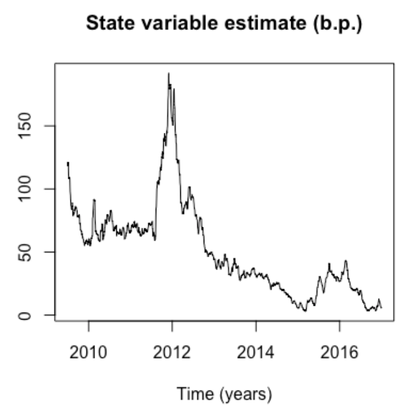

Figure 2: Estimate of λ_t^{ϕ}

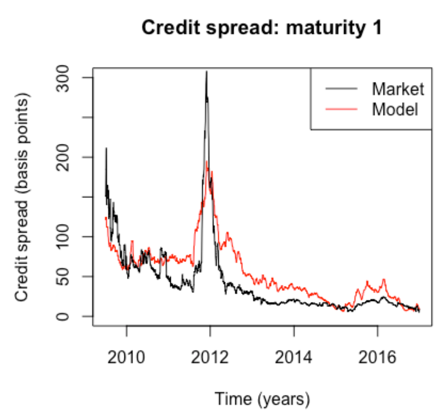

Figure 3: Comparison between historical and model credit spreads

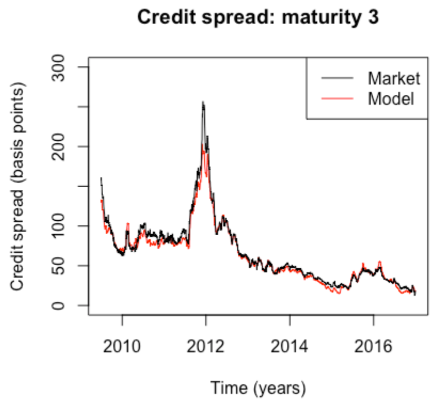

Figure 4: Comparison between historical and model credit spreads

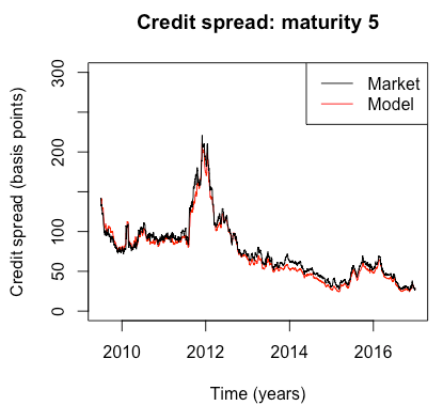

Figure 5: Comparison between historical and model credit spreads

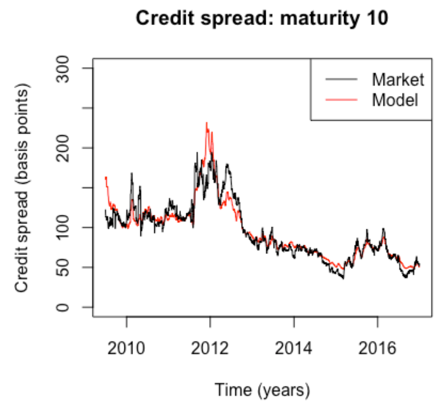

Figure 6: Comparison between historical and model credit spreads

Table 3: Means of historical market and model values

Maturity	Means MKT (b.p)	Means MDL (b.p.)
1	42.39	54.91
3	66.96	63.34
5	76.65	72.40
10	95.01	95.56

Table 4: Standard deviations of historical market and model values

Maturity	SD MKT (b.p)	SD MDL (b.p.)
1	44.01	36.35
3	40.94	36.26
5	36.28	36.02
10	36.09	35.47

Table 5: RMSE of the residuals

Maturity	RMSE (b.p)
1	26.79
3	8.45
5	6.51
10	13.40

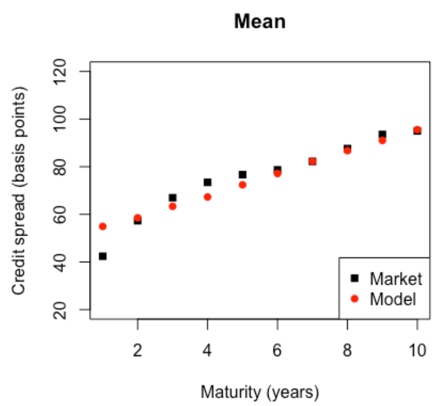

Figure 7: Mean analysis of historical and model credit spreads

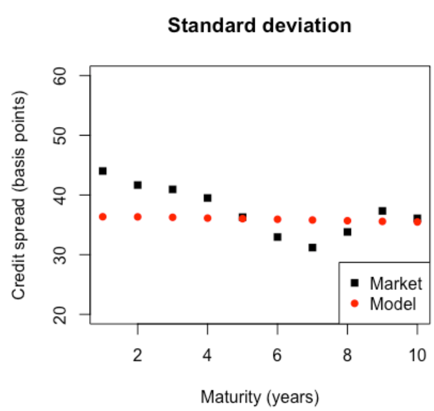

Figure 8: Standard deviation analysis of historical and model credit spreads

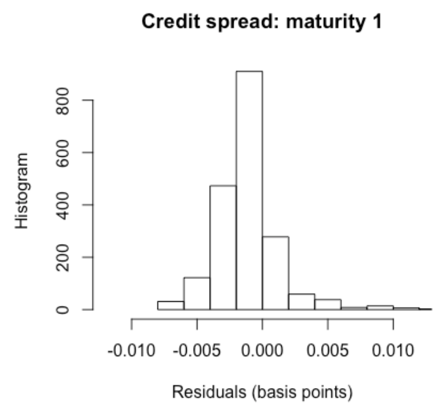

Figure 9: Distribution of the residuals: histogram

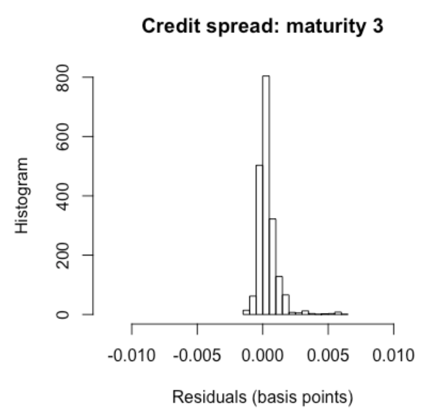

Figure 10: Distribution of the residuals: histogram

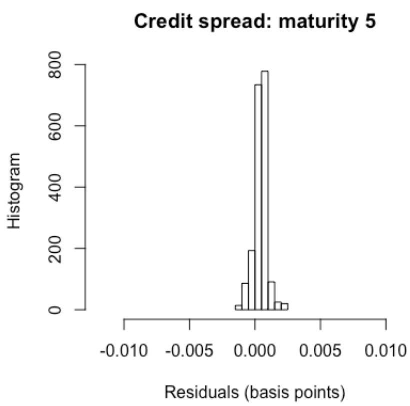

Figure 11: Distribution of the residuals: histogram

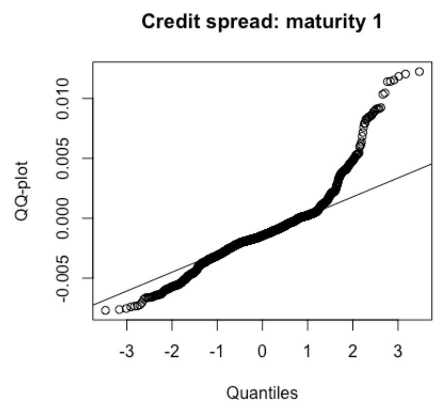

Figure 13: Distribution of the residuals: qq-plot

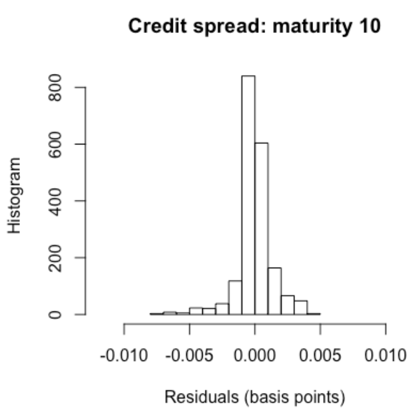

Figure 12: Distribution of the residuals: histogram

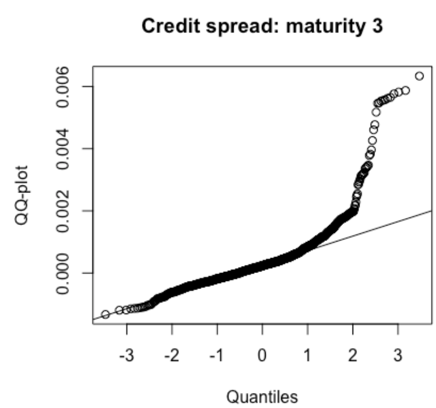

Figure 14: Distribution of the residuals: qq-plot

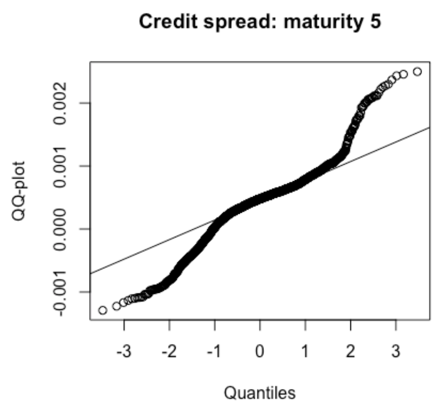

Figure 15: Distribution of the residuals: qq-plot

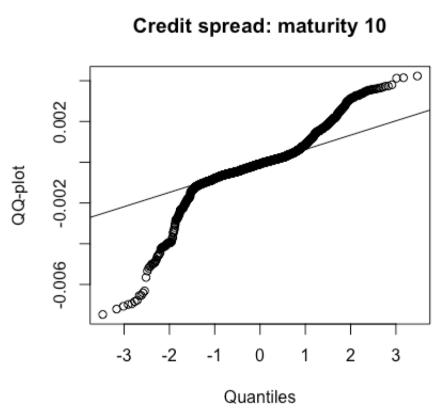

Figure 16: Distribution of the residuals: qq-plot